VAK 2024 MODERN ASTRONOMY: FROM THE EARLY UNIVERSE TO EXOPLANETS AND BLACK HOLES 300 years Russian Academy of Sciences

Study of the high-mass star-forming region S255IR at various scales

I. Zinchenko[1], S. Liu[2], D. Ojha[3], Y. Su[2], and P. Zemlyanukha[1]

[1] Federal Research Center A.V. Gaponov-Grekhov Institute of Applied Physics of the Russian Academy of Sciences, 46 Ul'yanov str., Nizhny Novgorod, 603950 Russia
[2] Institute of Astronomy and Astrophysics, Academia Sinica, 11F of Astronomy-Mathematics Building, AS/NTU No. 1, Sec. 4, Roosevelt Rd, Taipei, 10617 Taiwan
[3] Department of Astronomy and Astrophysics of the Tata Institute of Fundamental Research, Homi Bhabha Road, Mumbai, 400005 India

Abstract. The core of S255IR-SMA1 contains the protostar NIRS3 with a mass of about $20\,M_\odot$. A few years ago, the first burst of luminosity for massive protostars, caused by an episodic accretion event, was recorded here. We have been studying this object for a long time with various instruments, including ALMA. The general morphology and kinematics of this area have been investigated. Disk-shaped structures, jets and outflows have been identified and studied in detail. We have recently observed this object with ALMA at a resolution an order of magnitude higher than previously achieved—about 15 milliarcseconds, corresponding to about 25 AU. This paper presents new results from the analysis of these data together with observations in other bands. The new data show an inhomogeneous disk structure, an ionized region around the protostar, and the presence of a jet observed in the submillimeter continuum consisting of individual knots whose orientation differs markedly from that on large scales. The submillimeter emission from the jet most likely represents bremsstrahlung from ionized gas. Based on observations of the lines of some molecules, the kinematics and physical properties of this region are discussed. Methanol maser emission associated with the jet is observed.

Keywords: stars: formation, massive; ISM: clouds, molecules; submillimeter: ISM; individual: S255IR

DOI: 10.26119/VAK2024.096

1 Introduction

There are still several competing scenarios for high mass star formation (e.g., Tan et al. 2014; Motte et al. 2018; Padoan et al. 2020; Rosen et al. 2020). A key question is whether this process is a scaled-up version of the low-mass star formation or is significantly different. Observations at different scales are essential to choose between different scenarios.

In recent years, much attention has been paid to the luminosity bursts of massive protostars, which are thought to be caused by episodic disk-mediated accretion events. There are theoretical models that predict such a behavior (e.g., Meyer et al. 2017, 2019). To date, several such bursts have been recorded (see the summary in Wolf et al. 2024). One of the first of them was the burst in S255IR NIRS3, observed at IR (Caratti O Garatti et al. 2017) and submillimeter (Liu et al. 2018) wavelengths and accompanied by the methanol maser flare (Moscadelli et al. 2017; Szymczak et al. 2018).

The large star-forming complex sandwiched between the evolved H II regions S255 and S257 (Ojha et al. 2011) is a well-known and actively studied area of high-mass star formation. It contains two major star-forming sites: S255IR and S255N. Here we focus on the first one.

The distance to S255IR is estimated to be $1.78^{+0.12}_{-0.11}$ kpc from the maser parallax measurements (Burns et al. 2016). It contains three major cores SMA1, SMA2 and SMA3 (Wang et al. 2011) and several smaller condensations (Zinchenko et al. 2020). The SMA1 core harbors about 20 $M_\odot$ protostar NIRS3 (Zinchenko et al. 2015). The mass is estimated from the bolometric luminosity of $3 \times 10^4\, L_\odot$ at the assumed distance. Here we summarize and discuss the main results of our investigations of this object.

2 Observational data

We have observed the S255IR area with several single-dish radio telescopes (IRAM 30-m, OSO 29-m, MPIfR 100-m radiotelescope in Effelsberg) and with radio interferometers (ALMA, GMRT, SMA, VLA). These observations include imaging in the continuum and in many molecular lines. The frequency coverage was from 600 MHz (GMRT) to 350 GHz (ALMA). The angular resolution ranged from 40 arcseconds (for single-dish observations) to 15 milliarcseconds (for ALMA observations). At the distance to S255IR, 1 arcsecond corresponds to 1800 AU. In addition, we combine our radio data with our and other available data in other bands, especially with IR observations.

3 Structure of S255IR at various scales

In Fig. 1 we present a composite image of the S255IR area (size about 1′ or 0.5 pc) in several lines and in the continuum.

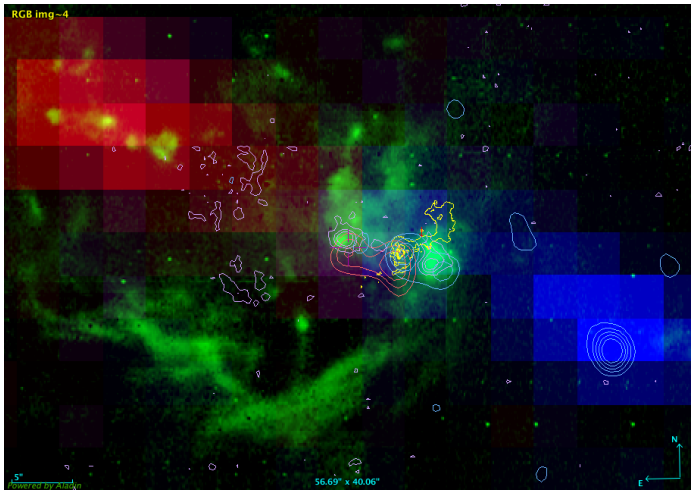

Fig. 1. S255IR area in the 2.12 μm H_2 line (green) and high-velocity CO(3–2) emission (red and blue). The yellow contours show the 0.9 mm emission (ALMA), the orange and blue contours show the high-velocity HCN(4–3) emission, the magenta contours show the 1.64 μm Fe II emission. The NIR data are from SINFONI observations (Wang et al. 2011). The radio data are from Zinchenko et al. (2012, 2015, 2020).

There are several H_2 knots aligned along the IR jet direction (PA $\approx 67°$) that were observed many years ago (Howard et al. 1997). The knots closest to S255IR-SMA1 also show strong Fe II emission and are associated with the high-velocity HCN(4–3) and HCO^+(4–3) emission (Zinchenko et al. 2015). These knots also coincide with the radio knots with non-thermal radio spectra (Obonyo et al. 2021). Apparently, these knots are associated with bow shocks and dense molecular gas. With the projected expansion velocity of about 450 km/s for the NE lobe (Fedriani et al. 2023; Cesaroni et al. 2023) and 285 km/s for the SW lobe (Cesaroni et al. 2024) their ejection happened about 60–70 years ago. Assuming the same velocity, the most distant knots were ejected several hundred years ago.

The distant H_2 NE knots coincide with the red-shifted CO(3–2) outflow lobe observed with the IRAM 30-m radio telescope (Fig. 1). The H_2 knots in the SW direction are less pronounced (although visible). The peak of the SW CO(3–2) outflow lobe coincides with the dense high-velocity clump seen in the HCN(4–3) and CS(7–6)

lines (Zinchenko et al. 2015). It is worth noting that there are two almost parallel outflows here, originating from the SMA1 and SMA2 cores (Zinchenko et al. 2020). The above connections suggest that the CO(3–2) outflow observed with the 30-m IRAM radio telescope originates from the SMA1 core.

Our ALMA observations at about 150 mas resolution show that this core represents a rotating and infalling envelope (pseudo-disk) around the NIRS3 protostar (Liu et al. 2020). In Fig. 2 we present some results from our latest (performed in September 2021) ALMA observations of this object at an order of magnitude higher resolution of about 15 mas, corresponding to 25 AU (Zinchenko et al., A&A, submitted).

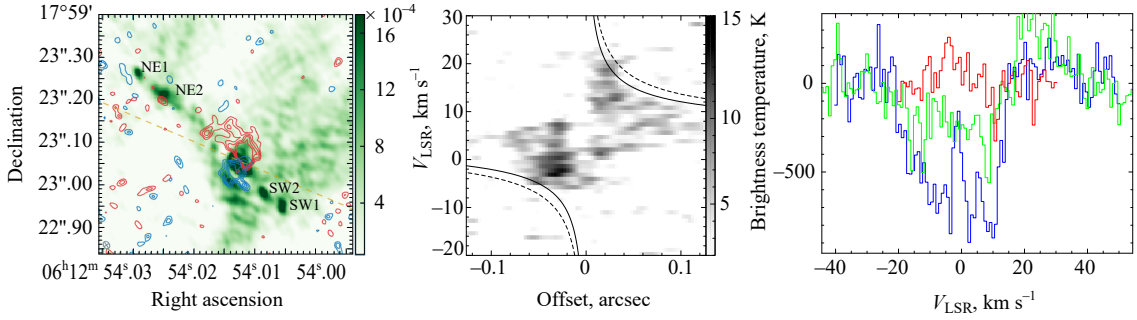

Fig. 2. Left panel: the image of the S255IR area in the continuum obtained with ALMA at 0.9 mm with about 15 mas resolution (Zinchenko et al., in preparation). The knots in the jet are marked. The red and blue contours show the emission in the $C^{34}S$(7–6) line wings. The dashed line indicates the jet orientation at larger scales (PA $\approx 67°$). Central panel: the PV diagram in the $C^{34}S$(7–6) line along the major axis of the disk. The curves correspond to the Keplerian rotation around the central mass of $M \sin^2 i = 10\,M_\odot$ (solid) and $M \sin^2 i = 15\,M_\odot$ (dashed), where i is the inclination angle. Right panel: spectra of the $C^{34}S$(7–6) (red), SiO(8–7) and CO(3–2) (blue) emission towards the central continuum peak.

The continuum image shows the central bright source (brightness temperature is about 850 K), which practically coincides with the NIRS3 position, and two pairs of bright knots (80–110 K), one pair in each outflow lobe, which is located almost on a straight line along with the central source. The position angle of this line is approximately 47°. Obviously, these knots belong to the jet emanating from the central source. Note that the central source is elongated approximately in the direction of the jet. The position angle of the jet differs by about 20° from that observed at larger scales (Fig. 2), as also found in some other observations at small scales (Hirota et al. 2021; Cesaroni et al. 2023). These results are consistent with the jet precession proposed in some previous works (Obonyo et al. 2021; Cesaroni et al. 2023). The

pairs of knots imply two ejection events with a time interval of about 1.5 yr. This is in good agreement with the 6.7 GHz methanol maser light curve (Szymczak et al. 2018).

The high brightness of the central source and its morphology imply a significant contribution of the free-free emission. Taking into account the flux measurements at lower frequencies from 3 GHz to 92 GHz (Obonyo et al. 2021; Cesaroni et al. 2023, 2024) we estimated the contributions of the ionized gas and dust emission assuming an optically thin free-free component. For the ionized gas we obtain the emission measure of $EM \sim 10^{10}\,\mathrm{pc/cm^6}$ and the electron density of $n_e \sim 10^7\,\mathrm{cm^{-3}}$. Such properties are typical of hypercompact H II regions. It is probably surrounded by a dust cocoon. An alternative model assumes a partially optically thick hypercompact H II region, which better explains the spectral index in the range 92–340 GHz. The emission from the knots in the jetappears to be dominated by the free-free component.

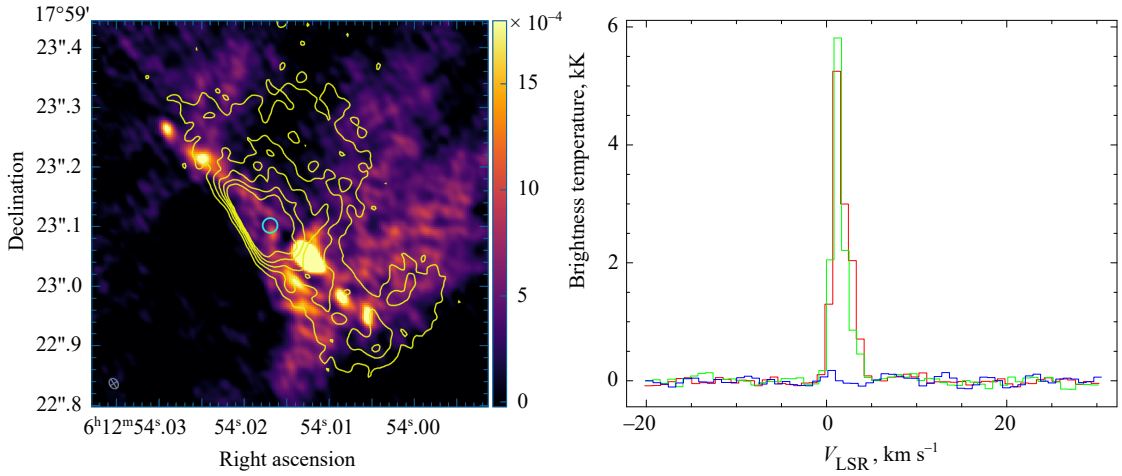

Fig. 3. Left panel: the continuum image of S255IR at 0.9 mm overlaid with contours of the CH_3OH 12_1–12_0 A^{-+} emission. Right panel: spectra of the CH_3OH 12_1–12_0 A^{-+} (red), 14_1–14_0 A^{-+} (green) and $^{13}CH_3OH$ 14_1–14_0 A^{-+} (blue) emission at the position marked by the circle.

Figure 2 shows a disk-like rotating structure around the central source. The molecular emission is very inhomogeneous, implying clumping. The PV diagrams in several lines (see an example in Fig. 2) indicate a sub-Keplerian rotation. There are also deep absorption features in the molecular spectra towards the bright central source. The deepest features are red-shifted relative to the systemic velocity of the core, suggesting an infall.

Previously we detected a new methanol maser line (14_1–14_0 A^{-+} at 349.1 GHz) toward S255IR-SMA1 (Zinchenko et al. 2017). In the new data, its intensity is consistent with the previous measurements, which show a decay since 2016 (Salii et al. 2022). Now there was another line of this series in the observed bands, 12_1–12_0 A^{-+}. It also shows the maser effect (Fig. 3). These masers are apparently associated with the jet and coincide with some other methanol masers recently discovered here (Baek et al. 2023).

4 Conclusions

In general, the observations of S255IR confirm the disk accretion scenario as the formation mechanism for about $20\,M_\odot$ stars. Further studies of its evolution after the recent accretion burst would be very important.

Funding

This work was supported by the Russian Science Foundation project No. 24-12-00153.

References

Baek G., Lee J., Evans N., et al., 2023, Astrophysical Journal Letters, 954, id. L25
Burns R., Handa T., Nagayama T., et al., 2016, MNRAS, 460, p. 283
Caratti O Garatti A., Stecklum B., Garcia Lopez R., et al., 2017, Nature Physics, 13, p. 276
Cesaroni R., Moscadelli L., Caratti o Garatti A., et al., 2023, Astron. & Astrophys., 680, p. A110
Cesaroni R., Moscadelli L., Caratti o Garatti A., et al., 2024, Astron. & Astrophys., 683, id. L15
Fedriani R., Caratti o Garatti A., Cesaroni R., et al., 2023, Astron. & Astrophys., 676, p. A107
Hirota T., Cesaroni R., Moscadelli L., et al., 2021, Astron. & Astrophys., 647, p. A23
Howard E.M., Pipher J.L., Forrest W.J. 1997, Astrophysical Journal, 481, p. 327
Liu S., Su Y., Zinchenko I., et al., 2020, Astrophysical Journal, 904, p. 181
Liu S., Su Y., Zinchenko I., et al., 2018, Astrophysical Journal, 863, id. L12
Meyer D., Vorobyov E., Elbakyan V., et al., 2019, MNRAS, 482, p. 5459
Meyer D., Vorobyov E., Kuiper R., et al., 2017, MNRAS, 464, id. L90
Moscadelli L., Sanna A., Goddi C., et al., 2017, Astron. & Astrophys., 600, id. L8
Motte F., Bontemps S., Louvet F. 2018, Annual Rev. Astron. Astrophys., 56, p. 41
Obonyo W., Lumsden S., Hoare M., et al., 2021, MNRAS, 501, p. 5197
Ojha D., Samal M., Pandey A., et al., 2011, Astrophysical Journal, 738, p. 156
Padoan P., Pan L., Juvela M., et al., 2020, Astrophysical Journal, 900, p. 82
Rosen A., Offner S., Sadavoy S., et al., 2020, Space Science Reviews, 216, p. 62
Salii S., Zinchenko I., Liu S., et al., 2022, MNRAS, 512, p. 3215
Szymczak M., Olech M., Wolak P., et al., 2018, Astron. & Astrophys., 617, p. A80
Tan J., Beltrán M., Caselli P., et al., 2014, Protostars and Planets VI, p. 149
Wang Y., Beuther H., Bik A., et al., 2011, Astron. & Astrophys., 527, p. A32
Wolf V., Stecklum B., Garatti A., et al., 2024, arXiv e-prints, arXiv:2405.10427
Zinchenko I., Liu S., Su Y., et al., 2012, Astrophysical Journal, 755, p. 177
Zinchenko I., Liu S., Su Y., et al., 2015, Astrophysical Journal, 810, p. 10
Zinchenko I., Liu S., Su Y., et al., 2017, Astron. & Astrophys., 606, id. L6
Zinchenko I., Liu S., Su Y., et al., 2020, Astrophysical Journal, 889, p. 43